Journal of Research in Pharmacy

Research Article

www.jrespharm.com

Design, synthesis, and biological evaluation of novel *N'*-(4-oxo-4*H*-chromen-3-yl) methylene propanehydrazides for Alzheimer's disease

Burcu KILIC [1] *

[1] Department of Pharmaceutical Chemistry, Faculty of Pharmacy, Gazi University, Ankara, Turkiye.
* Corresponding Author. E-mail: burcukahya@gazi.edu.tr (B.K.); Tel. +90-312-202 32 30.

Received: 21 July 2023 / Revised: 24 October 2023 / Accepted: 26 October 2023

ABSTRACT: Alzheimer's Disease (AD) is one of the most devastating chronic health problems of the last few decades. Unfortunately, current treatment and care options for AD are insufficient, making it a prominent topic for drug discovery studies. Currently, AD drug development studies have focused on the strategy of multitarget directed ligands (MTDLs). Following this strategy, we designed new ChE inhibitors with additional antioxidant and metal chelator effects. In this research, we designed and synthesized novel eight *N'*-(4-oxo-4H-chromen-3-yl)methylene propanehydrazide derivatives. We then evaluated the inhibition potency of all final compounds for cholinesterase enzymes. Among them, (**6f**) (*IC50* AChE=16.91 µM) was found to be the most potent acetylcholinesterase inhibitor. Additionally, (**6d**) (*IC50*'s AChE=26.91 µM and BChE=47.94 µM) exhibited dual cholinesterase inhibitor activity. Moreover, we investigated all title compounds for their antioxidant (DPPH, ORAC) and metal chelator activities. According to the ORAC-FL results, all the compounds exhibited good antioxidant activity ranging from 4.082 to 16.715 Trolox equivalents. We also observed chelator effects of all compounds for Cu(II), Fe(II), and Zn(II) ions at varying rates. Furthermore, we assessed the in-silico physicochemical parameters of the compounds to evaluate their drug-likeness or druggability.

KEYWORDS: Chromene; cholinesterase inhibition; antioxidant; metal-chelator; alzheimer's disease.

1. INTRODUCTION

Alzheimer's Disease (AD) is one of the most socially and economically devastating chronic health problems of the last few decades [1]. During the past two decades, there has been a rise in the number of deaths caused by AD. While deaths from other major causes decreased or remained stable, official records indicate a rise in deaths from AD during the two decades before the COVID-19 pandemic. Furthermore, in 2020-2021, the number of excess deaths from AD far exceeded what would be expected based on the normal trend line. COVID-19 most likely contributed to the sharp increase in AD deaths. This indicates that older adults with AD and other dementias are a vulnerable population, especially during extraordinary times like the pandemic. These findings highlight the inefficiency of current AD treatment and care options [2].

There are various pathophysiological hallmarks of AD have all been identified. Such as acetylcholine (ACh) deficiency, neuroinflammation, oxidative stress, metal ion dyshomeostasis, and protein dysregulations (amyloid-β (Aβ) aggregation and tau hyperphosphorylation) [3-5]. However, the exact underlying etiology of AD is still unclear. Therefore, AD continues to lack a definitive cure, making it a prominent focus in the ongoing efforts of drug discovery. In recent years, AD drug development studies have shifted towards MTDL (multitarget-directed ligands) strategy, moving away from the "one-target, one-drug" approach [6]. Based on the current understanding of AD, cholinesterase (ChE) inhibition is considered a crucial and practical target for MTDL design. Cognitive deficiency in AD related to the decreased levels of ACh. To overcome the clinical problems originating from ACh deficiency, acetylcholinesterase (AChE) and butyrylcholinesterase (BChE) inhibitors are always needed. Previously, AChE received more attention due to its additional non-catalytic feature. AChE possesses a more hydrophobic peripheral aromatic site (PAS) compared to BChE, enabling its interaction with peptides, and thus playing an accelerating role in Aβ pathophysiology. Nonetheless, recent studies suggest that AChE is selectively and mainly responsible for ACh hydrolysis in the healthy brain or during the initial stages of AD. As the disease progresses in the AD brain, activity of the BChE increases and takes over the role of AChE [7, 8]. Consequently, BChE inhibition

How to cite this article: Kilic B. Design, synthesis, and biological evaluation of novel *N'*-(4-oxo-4H-chromen-3-yl)methylene propanehydrazides for Alzheimer's disease. J Res Pharm. 2024; 28(5): 1344-1356.

ISSN: 2630-6344

http://dx.doi.org/10.29228/jrp.813

has gained more attention in recent AD drug development studies [9, 10]. Therefore, cholinesterases continue to be principal biological targets for the development of MTDLs, typically combining cholinesterase inhibitory activity with activity against disease-modifying or neuroprotective targets [11].

On the other hand, oxidative stress (OS) has been reported as one of the initial and triggering pathophysiologies of AD. It is also an important contributor to neurodegeneration through the damage it inflicts on biological macromolecules. Consequently, OS is a pivotal player in the progression of AD and closely associated with other pathophysiological pathways of the disease [12, 13]. Therefore, compounds with antioxidant activity are considered valuable for the design of multitarget-directed ligands (MTDLs) against AD.

The increasing body of evidence suggests that metal dysregulation is also implicated in the intricate and associated pathogenic network of AD. Fe, Cu, and Zn ions are important according to the metal hypothesis, because these three transition metals have been linked to OS, Aβ, and tau pathologies in AD [14]. Due to their synergistic effects on various mechanisms of AD, metal chelators are also considered valuable for drug development studies.

The core ring, chromone is a heterocyclic system found in many natural components of human and animal nutrition. It exhibits low toxicity for mammalian cells and synthetic chromone derivatives have become a privileged ring system in new drug development studies. These derivatives possess a broad spectrum of biological effects, including antibacterial, antifungal, antioxidant, antimalarial, antiviral, neuroprotective, antiulcer, and anti-inflammatory, anti-allergic activities [15]. Moreover, the chromone ring is also present in the structure of flavonoids, which are biologically active phytochemicals. Various flavonoids, such as genistein, apigenin, and acacetin, have been reported to have protective effects on neurodegenerative diseases through different mechanisms [16]. Notably, there are numerous natural compounds containing various chromone derivatives in their structure that have been reported as cholinesterase inhibitors [17]. Additionally, there are various publications in the literature in which chromone or its isomer coumarin was recruited for the anti-AD drug design [18-22]. Overall, the chromone ring is a preferred scaffold for designing enzyme inhibitors and multitarget-directed ligands (MTDLs), particularly for neurodegenerative diseases such as AD and Parkinson's Disease [23].

In the current work, our goal was to develop novel ChE inhibitors with additional antioxidant and metal chelator effects using the above-mentioned data and the MTDL approach. During last decade, our research team has focused to reach MTDLs against AD. With this aim, we have studied various heterocyclic scaffolds such as phthalazinone, pyridazinone, pyridazine, benzoxazolone, benzothiazolone, and thiazole [24-30]. Parallelly to our previous efforts, in this study, we combined the other versatile heterocycle, Chromone, recognized as a privileged scaffold for AD [23], with tertiary nitrogen-bearing structures known for their ability to interact with the catalytic site of cholinesterase enzymes [31, 32]. These two components were connected through a propanehydrazide bridge, which could contribute to the antioxidant and metal chelator effects [33]. As a result, we designed and synthesized novel eight *N'*-(4-oxo-4*H*-chromen-3-yl)methylene propanehydrazide derivatives (Figure 1). Subsequently, we evaluated their biological activity, including their inhibitory effects on cholinesterases, as well as their antioxidant and metal chelator properties. Additionally, *in silico* ADME predictions were performed to assess the drug-likeness of the compounds.

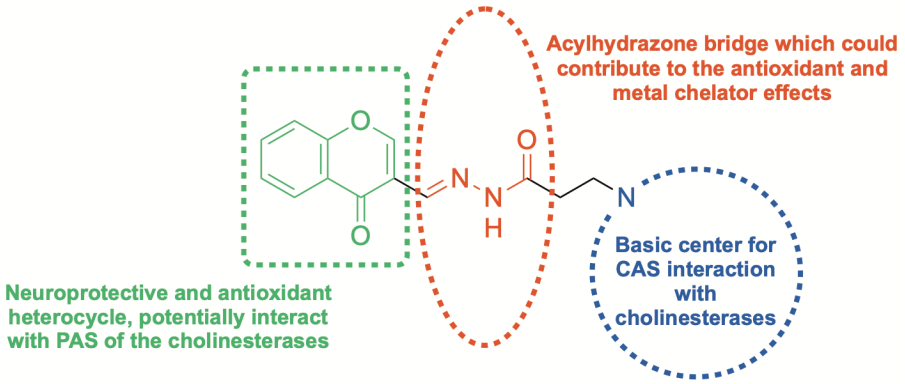

Figure 1. Design strategy and general structures of the final compounds

2. RESULTS and DISCUSSION

2.1. Chemistry

Route for the synthesis of intermediate and final compounds (**6a-h**) were presented in Figure 2. To begin, starting compound 4-oxo-4*H*-chromene-3-carbaldehyde (**2**) was synthesized by utilizing the commercially available 1-(2-hydroxyphenyl)ethan-1-one (**1**), phosphorus oxychloride and dimethyl formamide [34]. Subsequently, methyl 3-(substitutedamino)propanoate intermediates (**4a-h**) were prepared from the Michael addition of methyl acrylate and appropriate amine derivative (**3a-h**) [27]. Following that step, (**4a-h**) was refluxed in EtOH with hydrazine hydrate in order to obtain the corresponding 3-(substitutedamino)propane hydrazide intermediates (**5a-h**). Eventually, from the addition reaction of compounds (**2**) and (**5a-h**), *N'*-(4-oxo-4*H*-chromen-3-yl)methylene derivatives (**6a-h**) were synthesized.

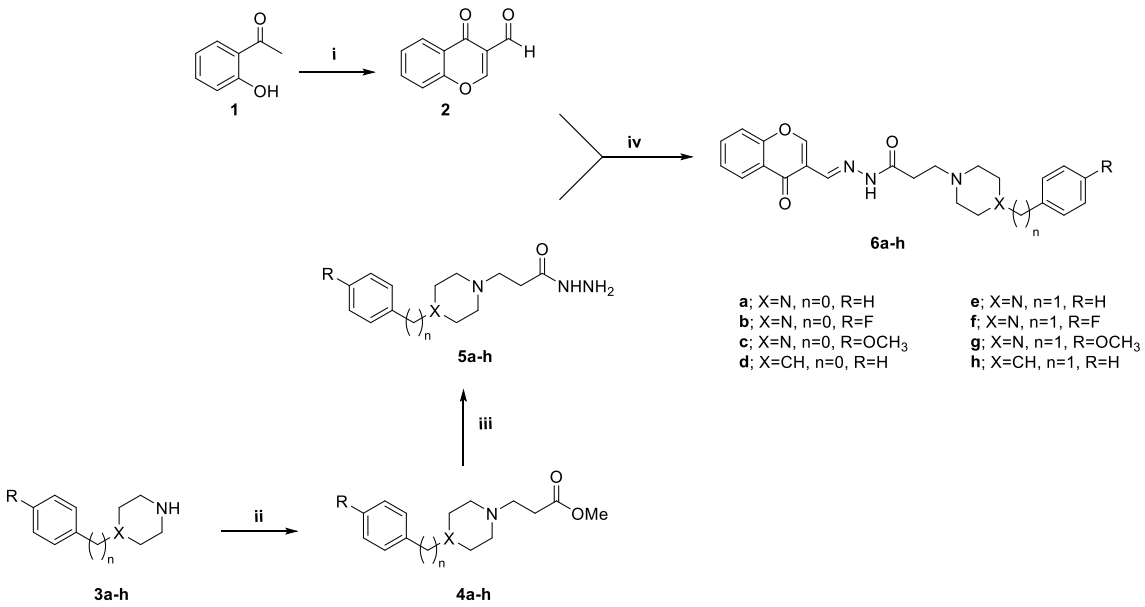

Figure 2. Synthesis of chromone derivatives **6a-h**. Reagents and conditions: (**i**) $POCl_3$, DMF, rt, overnight; (**ii**) Methyl acrylate, DCM, rt, 24h; (**iii**) Hydrazine monohydrate, EtOH, reflux, 4h; (**iv**) EtOH, reflux or rt.

Eight final compounds were synthesized in this study. ^{1}H NMR and high-resolution mass spectra (HRMS) were used for the chemical structure verification of the compounds. Additionally, ^{13}C NMR data of the (**6a)** was presented as a representative of the series. The data obtained from all analyses of the compounds matched the proposed structures.

Acylhydrazones, in other words, (-C(O)-N-N=C<) structure can potentially have *E/Z* geometrical isomers (C=N), *cis/trans* amide conformers (C(O)-NH), and rotational isomers (N-N). However, the presence of $Z_{(N\text{-}N)}$ conformations is unlikely because of steric crowding of the acyl group and chromene, as well as co-planarity and eclipsing of the acyl and amide bonds [35]. Additionally, in the solid form, *N*-acyl hydrazones of aromatic aldehydes typically adopt the *E* configuration, and the less hindered *E* conformation is also favored in solution. However, in less polar solvents like chloroform, the *Z* isomer can be detected [36]. Geometric isomers display considerably distinct *Rf* (retention factor) values. During the characterization of title compounds with TLC and LC-MS techniques, only the presence of *E* isomers was confirmed. According to afore mentioned-knowledge, possible isoforms of representative compound (**6a**) in NMR solvent $CDCl_3$ were illustrated in Figure 3. As a result of diastereomeric nature of the compounds (*E/Z*, *synperiplanar* and *antiperiplanar*), explicit sets of certain protons were observed in ^{1}H NMR spectra with a similar pattern for all compounds. Additionally, to simplify the evaluation of spectral data, ^{1}H NMR in DMSO-d_6 of (**6a**) was obtained. A comparison of $CDCl_3$ and DMSO-d_6 spectra revealed that the paired NMR peaks were mainly caused by *synperiplanar* (*sp*) and *antiperiplanar* (*ap*) conformers. In $CDCl_3$, the emergence of the *Z* isomer caused additional multiplicity of some paired peaks, especially aromatic ones. ^{13}C NMR spectra of the (**6a**) also exhibited duplicated signals because of the same reason.

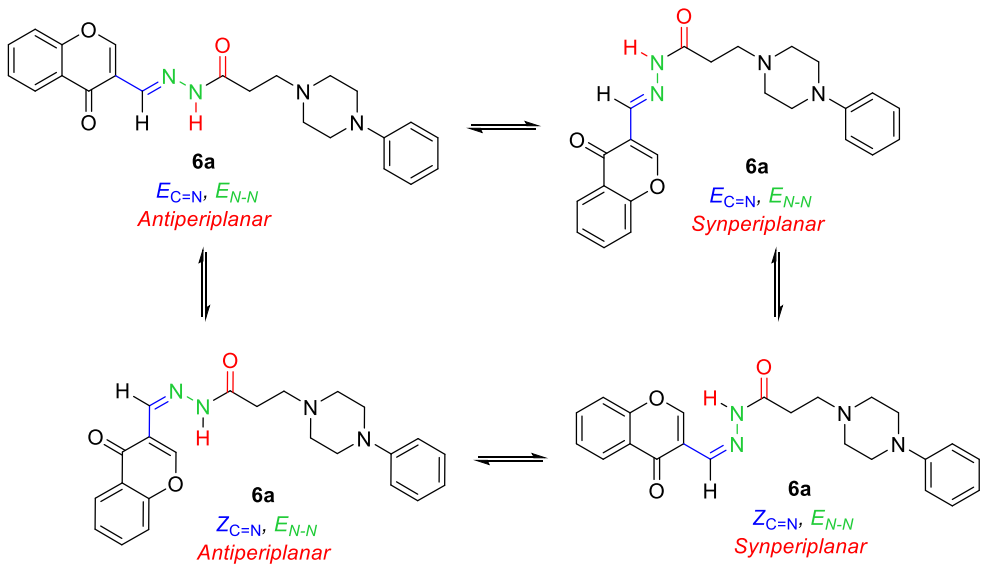

Figure 3. Possible isoforms of **6a** in NMR solvent $CDCl_3$.

2.2. Biological assays

2.2.1. Cholinesterase inhibition assay

By using modified Ellman's method, inhibition percentages of compounds on cholinesterases were evaluated at 10 and 100 µM. Subsequently, the *IC50*s of the final compounds were assayed and calculated. All the cholinesterase (ChE) inhibitory activity results were presented in Table 1. Among the tested compounds, (**6d**) (*IC50*'s AChE=26.91 µM and BChE=47.94 µM), (**6e**) (*IC50* AChE=17.59 µM), (**6f**) (*IC50* AChE=16.91 µM), and (**6h**) (*IC50*'s AChE=31.62 µM and BChE=86.32 µM) exhibited moderate ChE inhibitory activity. As a general structure–activity relationship (SAR) comment, benzyl-substituted tertiary amine derivatives (**6e-h**) were found to be more active compared to phenyl-substituted tertiary amine derivatives (**6a-d**). Exceptionally, only (**6d**) (with 4-phenyl piperidine) exhibited ChE inhibitory activity among the phenyl-substituted tertiary amine derivatives. According to these findings, the basicity of the tertiary amine atom at the third position of the propane hydrazide chain (piperazine N1 or piperidine N) may be responsible for ChE inhibition. However, for the benzyl derivatives, the p-methoxy substitution at the phenyl ring (**6g**) caused the disappearance of the ChE inhibitor activity. Possibly, the loss of activity resulted from the steric hindrance of the methoxy substituent. In terms of ChE inhibitory selectivity, compounds (**6d**) and (**6h**) were found to possess dual ChE inhibitory activity. But, their AChE selectivity was relatively higher compared to BChE.

Table 1. Cholinesterase inhibitory activity results of the synthesized compounds.

Compound	*ee*AChE			*eq*BChE		
	%inhibition (10 µM)	%inhibition (100 µM)	*IC50* (µM)	%inhibition (10 µM)	%inhibition (100 µM)	*IC50* (µM)
6a	≤10	≤10	≥100	≤10	≤10	≥100
6b	≤10	≤10	≥100	≤10	≤10	≥100
6c	≤10	≤10	≥100	≤10	≤10	≥100
6d	21.7 ± 8.4	63.7 ± 0.5	26.91 ± 0.13	32.8 ± 7.2	83.9 ± 0.6	47.94 ± 0.02
6e	20.1 ± 6.2	74.8 ± 3.8	17.59 ± 0.07	≤10	32.5 ± 8.5	≥100
6f	19.4 ± 3.2	71.8 ± 1.6	16.91 ± 0.06	≤10	42.8 ± 2.4	≥100
6g	≤10	≤10	≥100	≤10	12.5 ± 0.3	≥100
6h	16.2 ± 4.5	67.1 ± 5.1	31.62 ± 0.03	≤10	61.1 ± 5.1	86.32 ± 0.04
Donepezil	98.5 ± 0.1	-	0.062 ± 0.002	90.1 ± 1.1	-	3.55 ± 0.07
Galantamine	92.1 ± 1.1	-	nd	31.5 ± 1.8	-	nd

The mean ± SD of three independent experiments. n.d; not determined.

2.2.2. In vitro antioxidant activity (DPPH and ORAC-Fluorescein assay)

Compounds were tested for radical scavenging as well as oxygen radical absorbance. DPPH and ORAC-FL methods were recruited for antioxidant activity evaluation, respectively. Results are presented in Table 2. All compounds exhibited mild radical scavenging activity within the range of %8.41–30.27 at 100 µM. Additionally, they demonstrated good ORAC-FL values ranging from 4.082 to 16.715 trolox equivalents. In other words, compounds were found to have an antioxidant effect of at least four times that of Trolox. Additionally, (**6a**) was determined to be a very potent antioxidant, with 16.7 times the activity of trolox.

Table 2. Antioxidant activity results of the synthesized compounds.

Compound	DPPH*	ORAC-FL**
6a	27.37 ± 0.43	16.715 ± 0.158
6b	23.65 ± 1.83	12.169 ± 0.457
6c	29.23 ± 3.19	8.967 ± 0.168
6d	20.94 ± 2.53	4.082 ± 0.309
6e	22.73 ± 1.81	5.480 ± 0.133
6f	30.27 ± 3.71	6.920 ± 0.206
6g	22.34 ± 1.77	5.376 ± 0.073
6h	8.41 ± 1.90	4.296 ± 0.213
Gallic acid	92.31 ± 0.46	nd
Trolox	nd	1.000

The mean ± SD of three independent experiments. nd; not determined.
*(%) reduction percentage of DPPH, compounds at 100 µM.
**Data are expressed as µmol of Trolox equivalent/µmol of tested compounds.

2.2.3. Metal binding studies

The absorptions in the 230-500 nm range of the compounds were screened in order to evaluate their Cu(II), Fe(II), and Zn(II) binding capacities. Spectra of all compounds were presented in Supplementary Material. Based on the UV-vis spectrophotometry method, any kind of variation in the spectra of the metal-treated ligand when compared to the spectra of the ligand alone is attributed to complexation [37]. The "difference UV-vis spectra" were re-plotted and presented in Figure 4. In order to obtain "difference UV-vis spectra", the absorbances of the metal and the ligand were individually subtracted from the absorbance of the metal-ligand mixture. We discovered that all compounds exhibited chelation with all tested ions, albeit at varying rates. Notably, (**6a**), (**6b**), and (**6c**) exhibited strong Cu(II) chelation. Additionally, (**6d**), (**6e**), and (**6f**) showed significant Fe(II) and Zn(II) chelation. The acylhydrazones have a strong coordination ability with metal ions. They are participate in metal ion chelation via the keto-enol tautomerism, the electron donor (the oxygen atom of the carbonyl group) and the azomethine nitrogen atom (-N=) [38-40]. According to this knowledge, possible 1:1 chelate structures of the compounds could be as shown in Figure 5.

Journal of Research in Pharmacy
Research Article

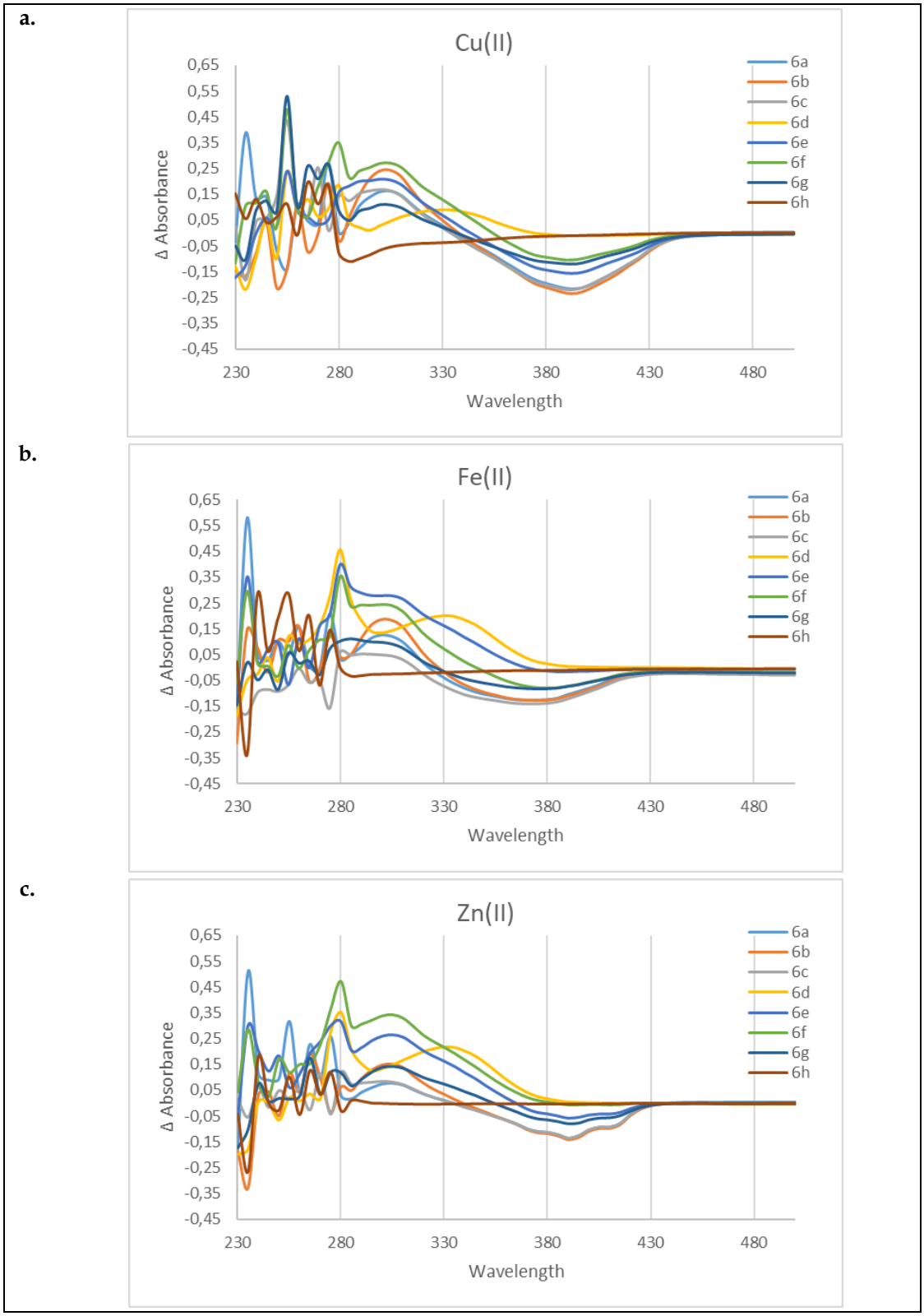

Figure 4. The difference UV–vis spectra between title compounds and Cu(II) (**a**), Fe(II) (**b**), Zn(II) (**c**) ions.

Figure 5. Possible structures for metal ion-compound interaction

http://dx.doi.org/10.29228/jrp.813
J Res Pharm 2024; 28(5): 1344-1356

2.3. Evaluation of *in silico* physicochemical parameters

For the calculation of in-silico physicochemical properties and ADME predictions QikProp, Schrodinger Suite 2021 was used [41]. The results are presented in Table 3. With QPlogBB values ranging from -0.689 to -0.156, all of the compounds were predicted to be BBB-permeable. Additionally, all compounds were forecasted to exhibit a CNS score of 1, falling within the range of -2 (inactive) to +2 (active). There were no violations of Lipinski's rule of five and Jorgensen's rule of three found in any of the compounds. Finally, *in silico* ADME predictions revealed that the compounds have acceptable drug-likeness as well as significant BBB permeation capacity.

Table 3. In-silico physicochemical properties and ADME predictions of compounds.

Descriptor/ ADME parameter	Compounds								VR*
	6a	6b	6c	6d	6e	6f	6g	6h	
MW	404.468	422.458	434.494	403.480	418.494	436.485	448.521	417.507	130 - 725
vol	1300.444	1317.029	1368.243	1310.862	1377.757	1393.639	1424.761	1376.887	500 - 2000
n-rot	6	6	7	6	8	8	9	8	0 - 15
DHB	1	1	1	1	1	1	1	1	0 - 6
AHB	8	8	8.75	7	9	9	9.75	7	2 - 20
PSA	89.611	89.602	101.303	83.339	93.196	93.195	97.415	87.899	7 - 200
QPlogS	-4.449	-4.841	-4.492	-4.940	-3.408	-3.765	-3.020	-5.335	-6.5 - 0.5
$QlogP_{o/w}$	3.436	3.672	3.373	3.937	2.755	2.987	2.861	4.226	2.0 - 6.5
QPCaco	370.778	370.925	281.584	385.048	49.998	49.998	90.868	261.915	<25 poor, >500 great
QlogBB	-0.342	-0.239	-0.548	-0.328	-0.444	-0.338	-0.156	-0.689	-3.0 - 1.2
CNS	1	1	1	1	1	1	1	1	-2 (inactive) to +2 (active)
#metab	2	2	3	4	4	4	5	3	1 - 8
%HOA	93.043	94.430	90.537	96.275	73.482	74.842	78.748	94.970	>80% is high <25% is poor
VRF	0	0	0	0	0	0	0	0	-
VJR	0	0	0	0	0	0	0	0	-

MW: Molecular weight **vol:** Total solvent-accessible volume **n-rot:** Number of rotatable bonds **DHB:** Estimated number of hydrogen bond donors **AHB:** Estimated number of hydrogen bond acceptors (2.0-20.0) **PSA:** Van der Waals surface area of polar nitrogen and oxygen atoms and carbonyl carbon atoms **QPlogS:** Predicted aqueous solubility **QlogPo/w:** Predicted octanol/water partition coefficient **QPCaco:** Predicted apparent Caco-2 cell permeability **QlogBB:** Predicted brain/blood partition coefficient **CNS:** Predicted central nervous system activity **#metab:** Number of likely metabolic reactions.%**HOA:**Predicted human oral absorption percent **VRF:** Number of violations of Lipinski's rule of five (The rules are: MW < 500, logP <5, DHB ≤ 5, AHB ≤ 10) **VJR:** Number of violations of Jorgensen's rule of three (QPlogS > -5.7, QP PCaco > 22 nm/s, # Primary Metabolites < 7).
*VR = gap or recommended value for 95% of known drugs (Schrödinger 2021-3 Release QikProp Manual User)

3. CONCLUSION

From the ChE inhibitory activity results, four out of the eight title compounds (**6d**, **6e**, **6f**, and **6h**) exhibited moderate AChE inhibition (*IC50*s range of from 16.91 to 31.62 μM). Two of them (**6d**, **6h**) also have moderate BChE inhibition (*IC50*s 47.94 and 86.32 μM). When we move to the antioxidant activity results, compounds exhibited good oxygen radical absorbance capacity (ORAC-FL values; 4.082–16.715). Unfortunately, their DPPH results showed only mild radical scavenging activity. Moreover, metal binding studies indicated that all the compounds were chelators for copper, iron, and zinc ions. Notably, based on in-silico predictions, compounds demonstrated appreciable BBB permeation capacity along with acceptable drug-likeness. Considering the multifunctional properties of **6d**, **6e**, **6f**, and **6h** they can be promising potential leads for further studies. To obtain more active compounds, we are planning to try structural modifications such as substituent addition to 4-oxo-*4H*-chromene ring and/or bioisosteric replacement of chromene ring. Overall, the *N'*-(4-oxo-4H-chromen-3-yl)methylene propanehydrazide structure could be considered as an attractive core structure for MTDL design against AD.

4. MATERIALS AND METHODS

4.1. Chemistry

Chemicals were acquired from commercial suppliers and Merck 60F254 plates were used for TLC. Schmelzpunkt SMP-II digital apparatus was used for melting point (mp) detection. NMR spectra were recorded using a Bruker Avance Neo 500 MHz FT-NMR spectrometer. Waters LCT Premier XE Mass Spectrometer operating in electrospray ionization (ESI) mode recruited to collect high resolution mass spectra data (HRMS). The mass spectrometer was also coupled to an AQUITY Ultra Performance Liquid Chromatography system with UV detector monitoring at 254 nm.

4.1.1. 4-Oxo-4H-chromene-3-carbaldehyde (2)

Starting compound **2** was synthesized from commercially available 1-(2-hydroxyphenyl)ethan-1-one (**1**) (4.0 ml, 33.29 mmol) by using the previously reported method [34]. Yield: 72 %. Light yellow solid. mp: 152-153 ◦C. HR-ESI-MS (m/z) calcd for $C_{10}H_7O_3$ $[M+H]^+$ 175.0395, found 175.0396.

4.1.2. General synthesis method of 3-(substitutedamino)propanehydrazide intermediates (5a-h)

Corresponding amine derivative (**3a-h**) (1.0 g, 1 equivalent) in DCM (15 ml) and methyl acrylate (1.2 equivalent) were used to obtain methyl 3-(substitutedamino)propanoate intermediates (**4a-h**), by the method we previously reported [27] Without further purification prepared (**4a-h**) (1.0 equivalent) and $NH_2NH_2.H_2O$ (64%, 5.0 equivalent) were refluxed in EtOH (25 ml) for 4h. Final mixture was concentrated under reduced pressure at the end of this period, then treated with diethyl ether, and the precipitated crude intermediate (**5a-h**) was filtered off and crystallized or washed with the appropriate solvent.

3-(4-Phenylpiperazin-1-yl)propanehydrazide (**5a**)

Crystallization solvent, ethyl acetate-hexane. Yield: 69 %. Beige solid. mp: 121-123 °C. HR-ESI-MS (m/z) calcd for $C_{13}H_{21}N_4O$ $[M+H]^+$ 249.1715, found 249.1708.

3-(4-(4-Fluorophenyl)piperazin-1-yl)propanehydrazide (**5b**)

Crystallization solvent, ethyl acetate-hexane. Yield: 58 %. White solid. mp: 114-115 °C. HR-ESI-MS (m/z) calcd for $C_{13}H_{20}FN_4O$ $[M+H]^+$ 267.1621, found 267.1620.

3-(4-(4-Methoxyphenyl)piperazin-1-yl)propanehydrazide (**5c**)

Washed with diethyl ether-petroleum ether. Yield: 81 %. White solid. mp: 141-143 °C. HR-ESI-MS (m/z) calcd for $C_{14}H_{23}N_4O_2$ $[M+H]^+$ 279.1821, found 279.1812.

3-(4-Phenylpiperidin-1-yl)propanehydrazide (**5d**)

Washed with diethyl ether-petroleum ether. Yield: 87 %. Light pinky solid. mp: 112-114 °C. HR-ESI-MS (m/z) calcd for $C_{14}H_{22}N_3O$ $[M+H]^+$ 248.1763, found 248.1761.

3-(4-Benzylpiperazin-1-yl)propanehydrazide (**5e**)

Crystallization solvent, diisopropyl ether-isopropyl alcohol. Yield: 70 %. Light pinky solid. mp: 73-75 °C. HR-ESI-MS (m/z) calcd for $C_{14}H_{23}N_4O$ $[M+H]^+$ 263.1872, found 263.1875.

3-(4-(4-Fluorobenzyl)piperazin-1-yl)propanehydrazide (**5f**)

Washed with diethyl ether-petroleum ether. Yield: 46 %. White solid. mp: 58-60 °C. HR-ESI-MS (m/z) calcd for $C_{14}H_{22}FN_4O$ $[M+H]^+$ 281.1778, found 281.1777.

3-(4-(4-Methoxybenzyl)piperazin-1-yl)propanehydrazide (**5g**)

Washed with diethyl ether-diisopropyl ether. Yield: 86 %. Light pinky solid. mp: 84-86 °C. HR-ESI-MS (m/z) calcd for $C_{15}H_{25}N_4O_2$ $[M+H]^+$ 293.1978, found 293.1987.

3-(4-Benzylpiperidin-1-yl)propanehydrazide (**5h**)

Crystallization solvent, ethyl acetate. Yield: 43 %. Light pinky solid. mp: 110-112 °C. HR-ESI-MS (m/z) calcd for $C_{15}H_{24}N_3O$ $[M+H]^+$ 262.1919, found 262.1913.

4.1.3. General synthesis method of N'-(4-oxo-4H-chromen-3-yl)methylene propanehydrazide derivatives (6a-h)

4-Oxo-4*H*-chromene-3-carbaldehyde (**2**) (1.0 equivalent) and corresponding 3-(substitutedamino) propanehydrazide intermediate (**5a-h**) (1.0 equivalent) were dissolved in EtOH (20 ml). The mixture was

either stirred at room temperature or refluxed until the starting compounds were no longer present. After completion, the mixture was concentrated under vacuum. Subsequently, mixture of petroleum and diethyl ether was added to the flask. The precipitated solid was filtered off and recrystallized from the appropriate solvent.

_N_'-((4-oxo-4_H_-chromen-3-yl)methylene)-3-(4-phenylpiperazin-1-yl)propanehydrazide (6a)

As mentioned in the general method, compounds **2** (250 mg, 1.44 mmol) and **5a** (356 mg, 1.44 mmol) were refluxed for 1.5 h. Recrystallization with acetonitrile. Yield: 86 %. White crystals. mp: 198-200 °C. ^{1}H NMR (500 MHz, $CDCl_3$) δ (ppm): 12.03, 9.22 (two s, 1H, NH), 8.77, 8.59 (two s, 1H, H^2), 8.32, 8.24 (two dd, J = 8.0, 1.5 Hz, 1H, H^5), 8.28, 8.18 (two s, 1H, -N=CH-), 7.82 – 7.66 (m, 1H, H^7), 7.60 – 7.39 (m, 2H, H^6, H^8), 7.35 – 7.22 (m, 2H, $H^{3'}$, $H^{5'}$), 7.06 – 6.85 (m, 3H, $H^{2'}$, $H^{4'}$, $H^{6'}$), 3.35 – 3.25 (m, 4H, $H^{3piperazine}$, $H^{5piperazine}$), 3.03, 2.94 (two t, J = 7.3 Hz, 1H, -CH_2C=O), 2.83 – 2.60 (m, 6H, -CH_2-piperazine, $H^{2piperazine}$, $H^{6piperazine}$), 2.03, 1.94 (s and br s, 1H, -CH_2C=O). ^{1}H NMR (500 MHz, DMSO-d_6) δ (ppm): 11.54, 11.35 (two s, 1H, NH), 8.84, 8.77 (two s, 1H, H^2), 8.32-8.11 (m, 2H, H^5, -N=CH-), 7.85 (t, 1H, H^7), 7.71 (d, 1H, H^8), 7.55 (t, 1H, H^6), 7.22 – 7.17 (m, 2H, $H^{3'}$, $H^{5'}$), 6.92 (t, 2H, J = 9.0 Hz, $H^{2'}$, $H^{6'}$), 6.77 (m, 1H, $H^{4'}$), 3.18 – 3.05 (m, 4H, $H^{3piperazine}$, $H^{5piperazine}$), 2.84 (t, J = 7.2 Hz, 1H, -CH_2C=O), 2.73 – 2.65 (m, 2H, -CH_2-piperazine), 2.61 – 2.53 (m, 4H, $H^{2piperazine}$, $H^{6piperazine}$), 2.42 (t, J = 7.2 Hz, 1H, -CH_2C=O). ^{13}C NMR (125 MHz, $CDCl_3$) δ (ppm): 175.86, 173.52, 168.75, 156.29, 154.57, 153.46, 151.18, 150.76, 139.67, 135.83, 134.32, 134.20, 129.23, 129.14, 126.12, 126.04, 125.91, 123.92, 120.37, 119.88, 118.54, 118.30, 116.42, 116.18, 53.40, 53.34, 53.12, 52.54, 49.46, 49.01, 31.21, 30.33. ^{13}C NMR (125 MHz, DMSO-d_6) δ (ppm): 175.50, 175.39, 173.78, 167.97, 156.23, 154.81, 154.70, 151.18, 151.47, 138.87, 135.56, 135.15, 135.08, 129.36, 126.54, 126.49, 125.67, 125.65, 123.79, 123.75, 119.24, 119.20, 119.16, 118.94, 118.72, 115.81, 115.78, 54.11, 53.76, 53.06, 52.84, 48.62, 32.63, 30.22. HR-ESI-MS (m/z) calcd for $C_{23}H_{25}N_4O_3$ $[M+H]^+$ 405.1927, found 405.1932.

3-(4-(4-Fluorophenyl)piperazin-1-yl)-_N_'-((4-oxo-4_H_-chromen-3-yl)methylene)propanehydrazide (6b)

As mentioned in the general method, compounds **2** (200 mg, 1.15 mmol) and **5b** (306 mg, 1.15 mmol) were refluxed for 3 h. Recrystallization with isopropyl alcohol. Yield: 86 %. Beige crystals. mp: 202-203 °C. ^{1}H NMR (500 MHz, $CDCl_3$) δ (ppm): 11.98, 9.20 (two s, 1H, NH), 8.78, 8.59 (two s, 1H, H^2), 8.31, 8.24 (two dd, J = 8.0, 1.5 Hz, 1H, H^5), 8.28, 8.17 (two s, 1H, -N=CH-), 7.76 – 7.71 (m, 1H, H^7), 7.56 – 7.44 (m, 2H, H^6, H^8), 6.97 – 6.86 (m, 4H, $H^{2'}$, $H^{3'}$, $H^{5'}$, $H^{6'}$), 3.26 – 3.18 (m, 4H, $H^{3piperazine}$, $H^{5piperazine}$), 3.03, 2.95 (two t, J = 7.3 Hz, 1H, -CH_2C=O), 2.83 – 2.60 (m, 6H, -CH_2-piperazine, $H^{2piperazine}$, $H^{6piperazine}$), 2.06, 1.94 (s and br s, 1H, -CH_2C=O). HR-ESI-MS (m/z) calcd for $C_{23}H_{24}FN_4O_3$ $[M+H]^+$ 423.1832, found 423.1823.

3-(4-(4-Methoxyphenyl)piperazin-1-yl)-_N_'-((4-oxo-4_H_-chromen-3-yl)methylene)propanehydrazide (6c)

As mentioned in the general method, compounds **2** (250 mg, 1.44 mmol) and **5c** (405 mg, 1.44 mmol) were refluxed for 3h. Recrystallization with acetonitrile. Yield: 73 %. White crystals. mp: 188-189 °C. ^{1}H NMR (500 MHz, $CDCl_3$) δ (ppm): 12.07, 9.04 (two s, 1H, NH), 8.77, 8.60 (two s, 1H, H^2), 8.31, 8.25 (two dd, J = 8.0, 1.3 Hz, 1H, H^5), 8.28, 8.14 (two s, 1H, -N=CH-), 7.77 – 7.70 (m, 1H, H^7), 7.56 – 7.44 (m, 2H, H^6, H^8), 7.02 – 6.85 (m, 4H, $H^{2'}$, $H^{3'}$, $H^{5'}$, $H^{6'}$), 3.80, 3.78 (two s, 1H, -OCH_3), 3.23 – 3.18 (m, 4H, $H^{3piperazine}$, $H^{5piperazine}$), 3.06, 2.97 (two t, J = 6.8 Hz, 1H, -CH_2C=O), 2.82 – 2.63 (m, 6H, -CH_2-piperazine, $H^{2piperazine}$, $H^{6piperazine}$), 2.03, 1.87 (s and br s, 1H, -CH_2C=O). HR-ESI-MS (m/z) calcd for $C_{24}H_{27}N_4O_4$ $[M+H]^+$ 435.2032, found 435.2031.

_N_'-((4-oxo-4_H_-chromen-3-yl)methylene)-3-(4-phenylpiperidin-1-yl)propanehydrazide (6d)

As mentioned in the general method, compounds **2** (250 mg, 1.44 mmol) and **5d** (355 mg, 1.44 mmol) were stirred at rt for 2 h. Recrystallization with acetonitrile. Yield: 59 %. Salmon crystals. mp: 183-184 °C. ^{1}H NMR (500 MHz, $CDCl_3$) δ (ppm): 12.43, 8.97 (two s, 1H, NH), 8.80, 8.63 (two s, 1H, H^2), 8.35, 8.14 (two s, 1H, -N=CH-), 8.32 – 8.28 (m, 1H, H^5), 7.77 – 7.72 (m, 1H, H^7), 7.56 – 7.46 (m, 2H, H^6, H^8), 7.40 – 7.20 (m, 5H, $H^{2'}$, $H^{3'}$, $H^{4'}$, $H^{5'}$, $H^{6'}$), 3.23 (d, J = 11.8 Hz, 2H, $H^{2piperidine(eq)}$, $H^{6piperidine(eq)}$), 3.10, 2.96 (two distorted t, 1H, -CH_2C=O), 2.79 – 2.55 (m, 3H, -CH_2-piperidine, $H^{4piperidine}$), 2.27 (t, J = 11.8 Hz, 2H, $H^{2piperidine(ax)}$, $H^{6piperidine(ax)}$), 2.08 – 1.73 (m, 5H, H^3, H^5, -CH_2C=O). HR-ESI-MS (m/z) calcd for $C_{24}H_{26}N_3O_3$ $[M+H]^+$ 404.1974, found 404.1974.

3-(4-Benzylpiperazin-1-yl)-_N_'-((4-oxo-4_H_-chromen-3-yl)methylene)propanehydrazide (6e)

As mentioned in the general method, compounds **2** (250 mg, 1.44 mmol) and **5e** (377 mg, 1.44 mmol) were stirred at rt for overnight. Recrystallization with acetonitrile. Yield: 30 %. Light yellow crystals. mp: 163-164 °C. ^{1}H NMR (500 MHz, $CDCl_3$) δ (ppm): 12.32, 8.90 (two s, 1H, NH), 8.80, 8.58 (two s, 1H, H^2), 8.31, 8.10 (two s, 1H, -N=CH-), 8.30 – 8.28 (m, 1H, H^5), 7.75 (ddd, J = 8.5, 7.2, 1.7 Hz, 1H, H^7), 7.55 (d, J = 8.3 Hz, 1H, H^8), 7.49 (t, J = 7.6 Hz, 1H, H^6), 7.40 – 7.25 (m, 5H, $H^{2'}$, $H^{3'}$, $H^{4'}$, $H^{5'}$, $H^{6'}$), 3.59, 3.57 (two s, 2H, piperazine-

CH_2-phenyl), 3.02, 2.91 (two distorted t, 1H, -CH_2C=O) 2.80 – 2.34 (m, 10H, -CH_2-piperazine, piperazine), 2.03, 1.84 (s and br s, 1H, -CH_2C=O). HR-ESI-MS (m/z) calcd for $C_{24}H_{27}N_4O_3$ $[M+H]^+$ 419.2083, found 419.2086.

3-(4-(4-Fluorobenzyl)piperazin-1-yl)-*N*'-((4-oxo-4*H*-chromen-3-yl)methylene)propanehydrazide (6f)

As mentioned in the general method, compounds **2** (250 mg, 1.44 mmol) and **5f** (402 mg, 1.44 mmol) were stirred at rt for overnight. Recrystallization with acetonitrile. Yield: 51 %. Beige crystals. mp: 171-172 °C. ^{1}H NMR (500 MHz, $CDCl_3$) δ (ppm): 12.29, 8.94 (two s, 1H, NH), 8.80, 8.58 (two s, 1H, H^2), 8.30, 8.11 (two s, 1H, -N=CH-), 8.30 – 8.28 (m, 1H, H^5), 7.75 (ddd, *J* = 8.7, 7.2, 1.7 Hz, 1H, H^7), 7.55 (d, *J* = 8.0 Hz, 1H, H^8), 7.49 (t, *J* = 7.6 Hz, 1H, H^6), 7.35 – 7.29 (m, 2H, $H^{2'}$, $H^{6'}$), 7.09 – 6.96 (m, 2H, $H^{3'}$, $H^{5'}$), 3.55, 3.52 (two s, 2H, piperazine-CH_2-phenyl), 3.05, 2.86 (two distorted t, 1H, -CH_2C=O), 2.82 – 2.30 (m, 10H, -CH_2-piperazine, piperazine), 2.03, 1.85 (s and br s, 1H, -CH_2C=O). HR-ESI-MS (m/z) calcd for $C_{24}H_{26}FN_4O_3$ $[M+H]^+$ 437.1989, found 437.1973.

3-(4-(4-Methoxybenzyl)piperazin-1-yl)-*N*'-((4-oxo-4*H*-chromen-3-yl)methylene)propanehydrazide (6g)

As mentioned in the general method, compounds **2** (250 mg, 1.44 mmol) and **5g** (416 mg, 1.44 mmol) were stirred at rt for overnight. Recrystallization with acetonitrile. Yield: 63 %. Beige crystals. mp: 165-166 °C. ^{1}H NMR (500 MHz, $CDCl_3$) δ (ppm): 12.35 (s, 1H, NH), 8.80, 8.55 (two s, 1H, H^2), 8.30 – 8.28 (m, 1H, H^5), 8.29, 8.07 (two s, 1H, -N=CH-), 7.75 (ddd, *J* = 8.7, 7.2, 1.7 Hz, 1H, H^7), 7.55 (d, *J* = 8.0 Hz, 1H, H^8), 7.49 (t, *J* = 7.6 Hz, 1H, H^6), 7.28 – 7.24 (m with $CDCl_3$, 2H, $H^{2'}$, $H^{6'}$), 6.89, 6.86 (d, *J* = 8.6 Hz, 2H, $H^{3'}$, $H^{5'}$), 3.82, 3.81 (s, 3H, -OCH_3), 3.52, 3.49 (s, 2H, piperazine-CH_2-phenyl), 2.99 – 2.81 (m, 1H, -CH_2C=O), 2.77 – 2.31 (m, 10H, -CH_2-piperazine, piperazine), 2.03, 1.73 (s and br s, 1H, -CH_2C=O). HR-ESI-MS (m/z) calcd for $C_{24}H_{27}N_4O_4$ $[M+H]^+$ 449.2189, found 449.2187.

3-(4-Benzylpiperidin-1-yl)-*N*'-((4-oxo-4*H*-chromen-3-yl)methylene)propanehydrazide (6h)

As mentioned in the general method, compounds **2** (300 mg, 1.72 mmol) and **5h** (448 mg, 1.72 mmol) were stirred at rt for 3.5h. Recrystallization with acetonitrile. Yield: 61 %. White crystals. mp: 177-178 °C. ^{1}H NMR (500 MHz, $CDCl_3$) δ (ppm): 12.49, (s, 1H, NH), 8.80, 8.61 (two s, 1H, H^2), 8.30 (dd, *J* = 8.0, 1.6 Hz, 1H, H^5), 8.28, 8.09 (two s, 1H, -N=CH-), 7.75 (ddd, *J* = 8.6, 7.2, 1.6 Hz, 1H, H^7), 7.55 (d, *J* = 8.4 Hz, 1H, H^8), 7.49 (t, *J* = 7.6 Hz, 1H, H^6), 7.35 – 7.26 (m with $CDCl_3$, 2H, $H^{3'}$, $H^{5'}$), 7.25 – 7.12 (m, 3H, $H^{2'}$, $H^{4'}$, $H^{6'}$), 3.07 (d, *J* = 11.4 Hz, 2H, $H^{2piperidine(eq)}$, $H^{6piperidine(eq)}$), 2.67 (t, *J* = 5.8 Hz, 2H, -CH_2C=O), 2.63 (d, *J* = 7.3 Hz, 2H, piperidine-CH_2-phenyl), 2.56 (t, *J* = 5.8 Hz, 2H, -CH_2-piperidine), 2.06 (t, *J* = 11.4 Hz, 2H, $H^{2piperidine(ax)}$, $H^{6piperidine(ax)}$), 1.80 (d, *J* = 12.8 Hz, 2H, $H^{3piperidine(eq)}$, $H^{5piperidine(eq)}$), 1.68 –1.56 (m, 1H, $H^{4piperidine)}$), 1.44 – 1.31 (m, 2H, $H^{3piperidine(ax)}$, $H^{5piperidine(ax)}$). HR-ESI-MS (m/z) calcd for $C_{25}H_{28}N_3O_3$ $[M+H]^+$ 418.2131, found 418.2136.

4.2. Biological assays

4.2.1. Cholinesterase inhibition assay

AChE (electric eel) and BChE (equine serum) from Sigma Aldrich were employed in the assays, following the method previously reported by us [24]. To determine the *IC50* values, GraphPad Prism software (Version 7.0) was used. Dose-response curves of the compounds were presented at Supplementary Material.

4.2.2. In vitro antioxidant activity (DPPH and ORAC-Fluorescein assay)

DPPH and ORAC-FL assays were conducted using our previously reported procedures [24]. In DPPH assay, test samples were assayed at 100 µM for 30 min incubation time. Assay was carried out in triplicate, and the mean±SD was computed.

4.2.3. Metal binding studies

Studies for the ligand-metal binding evaluation was carried out in accordance with our previously reported methodology [24]. The overlapping spectra of the metal-treated ligand and the control solution of the ligand were visualized, and the resulting wavelength (nm) vs. absorbance graphs were included in the supplementary data.

4.3. Evaluation of *in silico* physicochemical parameters

In order to obtain low energy conformations of the ligands as well as potential ionization states for pH 7.0 ± 2.0, LigPrep module was used. Table 3 shows the Qikprop predictions for the top-scoring states of each compound [41].

Acknowledgements: This study was supported by the Gazi University Scientific Research Projects Unit (Gazi BAP) under grant number THD-2023-8567. The author is grateful to Prof. Dr. Deniz S. Doğruer for her support and advice during this research.

Author contributions: Concept – B.K.; Design – B.K.; Supervision – B.K.; Resources – B.K.; Materials – B.K.; Data Collection and/or Processing – B.K.; Analysis and/or Interpretation – B.K.; Literature Search – B.K.; Writing – B.K.; Critical Reviews – B.K.

Conflict of interest statement: The authors declared no conflict of interest.

REFERENCES

[1] World Alzheimer Report 2019: Attitudes to Dementia. Alzheimer's Disease International (ADI) 2019. https://www.alzint.org/u/WorldAlzheimerReport2019.pdf (accessed on 23 October 2023).

[2] 2023 Alzheimer's disease facts and figures. Alzheimer's & Dementia. 2023; 19(4): 1598-1695. https://www.alz.org/media/documents/alzheimers-facts-and-figures.pdf (accessed on 23 October 2023).

[3] Kumar A, Singh A, Ekavali. A review on Alzheimer's disease pathophysiology and its management: An update. Pharmacol Rep. 2015; 67(2): 195-203. https://doi.org/10.1016/j.pharep.2014.09.004

[4] DeTure MA, Dickson DW. The neuropathological diagnosis of Alzheimer's disease. Mol Neurodegener. 2019; 14(1): 32. https://doi.org/10.1186/s13024-019-0333-5

[5] Blaikie L, Kay G, Kong Thoo Lin P. Current and emerging therapeutic targets of alzheimer's disease for the design of multi-target directed ligands. MedChemComm. 2019; 10(12): 2052-2072. http://dx.doi.org/10.1039/C9MD00337A

[6] Cavalli A, Bolognesi ML, Minarini A, Rosini M, Tumiatti V, Recanatini M, Melchiorre C. Multi-target-directed ligands to combat neurodegenerative diseases. J Med Chem. 2008; 51(3): 347-372. https://doi.org/10.1021/jm7009364

[7] Li Q, Xing S, Chen Y, Liao Q, Xiong B, He S, Lu W, Liu Y, Yang H, Li Q, Feng F, Liu W, Chen Y, Sun H. Discovery and biological evaluation of a novel highly potent selective butyrylcholinsterase inhibitor. J Med Chem. 2020; 63(17): 10030-10044. https://doi.org/10.1021/acs.jmedchem.0c01129

[8] Chen Y, Lin H, Yang H, Tan R, Bian Y, Fu T, Wei Li, Wu L, Pei Y , Sun H. Discovery of new acetylcholinesterase and butyrylcholinesterase inhibitors through structure-based virtual screening. RSC Adv. 2017; 7(6): 3429-3438. https://doi.org/10.1039/c6ra25887e

[9] Jing L, Wu G, Kang D, Zhou Z, Song Y, Liu X, Zhan P. Contemporary medicinal-chemistry strategies for the discovery of selective butyrylcholinesterase inhibitors. Drug Discov Today. 2019; 24(2): 629-635. https://doi.org/10.1016/j.drudis.2018.11.012

[10] Panek D, Pasieka A, Latacz G, Zaręba P, Szczęch M, Godyń J, Chantegreil F, Nachon F, Brazzolotto X, Wiercioch AS, Walczak M, Smolik M, Sałat K, Höfner G, Wanner K, Więckowska A, Malawska B. Discovery of new, highly potent and selective inhibitors of BuChE - design, synthesis, in vitro and in vivo evaluation and crystallography studies. Eur J Med Chem. 2023; 249: 115135. https://doi.org/10.1016/j.ejmech.2023.115135

[11] Wichur T, Więckowska A, Więckowski K, Godyń J, Jończyk J, Valdivieso ÁdR, Panek D, Pasieka A, Sabaté R, Knez D, Gobec S, Malawska B. 1-Benzylpyrrolidine-3-amine-based BuChE inhibitors with anti-aggregating, antioxidant and metal-chelating properties as multifunctional agents against Alzheimer's disease. Eur J Med Chem. 2020; 187: 111916. https://doi.org/10.1016/j.ejmech.2019.111916

[12] Zhao Y, Zhao B. Oxidative stress and the pathogenesis of Alzheimer's disease. Oxid Med Cell Longev. 2013; 2013: 316523. https://doi.org/10.1155/2013/316523

[13] Singh A, Kukreti R, Saso L, Kukreti S. Oxidative Stress: A Key Modulator in Neurodegenerative Diseases. Molecules. 2019; 24(8):1583. https://doi.org/10.3390/molecules24081583

[14] Kenche VB, Barnham KJ. Alzheimer's disease & metals: therapeutic opportunities. Br J Pharmacol. 2011; 163(2): 211-219. https://doi.org/10.1111/j.1476-5381.2011.01221.x

[15] Mohsin NuA, Irfan M, Hassan Su, Saleem U. Current strategies in development of new chromone derivatives with diversified pharmacological activities: A review. Pharm Chem J. 2020; 54(3): 241-257. https://doi.org/10.1007/s11094-020-02187-x

[16] Hussain G, Zhang L, Rasul A, Anwar H, Sohail MU, Razzaq A, Aziz N, Shabbir A, Ali M, Sun T. Role of plant-derived flavonoids and their mechanism in attenuation of alzheimer's and Parkinson's Diseases: An update of recent data. Molecules. 2018; 23(4): 814. https://doi.org/10.3390/molecules23040814

[17] Costa M, Dias TA, Brito A, Proença F. Biological importance of structurally diversified chromenes. Eur J Med Chem. 2016; 123: 487-507. https://doi.org/10.1016/j.ejmech.2016.07.057

[18] Jiang N, Huang Q, Liu J, Liang N, Li Q, Li Q, Xie S. Design, synthesis and biological evaluation of new coumarin-dithiocarbamate hybrids as multifunctional agents for the treatment of Alzheimer's disease. Eur J Med Chem. 2018; 146: 287-298. https://doi.org/10.1016/j.ejmech.2018.01.055

[19] Jalili-Baleh L, Nadri H, Forootanfar H, Samzadeh-Kermani A, Küçükkılınç TT, Ayazgok B, Rahimifard M, Baeeri M, Doostmohammadi M, Firoozpour L, Nasir S, Bukhari A, MR Ganjali, Emami S, Khoobi M, Foroumadi A. Novel 3-phenylcoumarin–lipoic acid conjugates as multi-functional agents for potential treatment of Alzheimer's disease. Bioorg Chem. 2018; 79: 223-234. https://doi.org/10.1016/j.bioorg.2018.04.030

[20] Sun Q, Peng D-Y, Yang S-G, Zhu X-L, Yang W-C, Yang G-F. Syntheses of coumarin–tacrine hybrids as dual-site acetylcholinesterase inhibitors and their activity against butylcholinesterase, Aβ aggregation, and β-secretase. Bioorg Med Chem. 2014; 22(17): 4784-4791. https://doi.org/10.1016/j.bmc.2014.06.057

[21] Wang D, Hu M, Li X, Zhang D, Chen C, Fu J, Shao S, Shi G, Zhou Y, Wu S, Zhang T . Design, synthesis, and evaluation of isoflavone analogs as multifunctional agents for the treatment of Alzheimer's disease. Eur J Med Chem. 2019; 168: 207-220. https://doi.org/10.1016/j.ejmech.2019.02.053

[22] Estrada-Valencia M, Herrera-Arozamena C, Pérez C, Viña D, Morales-García JA, Pérez-Castillo A, Viña D, Garcia J, Castillo AP, Ramos E, Romeo A, Laurini E, Pricl S. New flavonoid – N,N-dibenzyl(N-methyl)amine hybrids: Multi-target-directed agents for Alzheimer´s disease endowed with neurogenic properties. J Enzyme Inhib Med Chem. 2019; 34(1): 712-727. https://doi.org/10.1080/14756366.2019.1581184

[23] Sharma K. Chromone scaffolds in the treatment of Alzheimer's and Parkinson's Disease: An overview. ChemistrySelect. 2022; 7(18): e202200540. https://doi.org/10.1002/slct.202200540

[24] Kilic B, Bardakkaya M, Ilıkcı Sagkan R, Aksakal F, Shakila S, Dogruer DS. New thiourea and benzamide derivatives of 2-aminothiazole as multi-target agents against Alzheimer's disease: Design, synthesis, and biological evaluation. Bioorg Chem. 2023; 131: 106322. https://doi.org/10.1016/j.bioorg.2022.106322

[25] Erdogan M, Kilic B, Sagkan RI, Aksakal F, Ercetin T, Gulcan HO, Dogruer DS. Design, synthesis and biological evaluation of new benzoxazolone/benzothiazolone derivatives as multi-target agents against Alzheimer's disease. Eur J Med Chem. 2021; 212: 113124. https://doi.org/10.1016/j.ejmech.2020.113124

[26] Kilic B, Erdogan M, Gulcan HO, Aksakarl F, Oruklu N, Bagriacik EU, Dogruer DS. Design, synthesis and investigation of new diphenyl substituted pyridazinone derivatives as both cholinesterase and a beta-aggregation inhibitors. Med Chem. 2019; 15(1): 59-76. https://dx.doi.org/10.2174/1573406414666180524073241

[27] Kilic B, Gulcan HO, Aksakal F, Ercetin T, Oruklu N, Umit Bagriacik E, Dogruer DS. Design and synthesis of some new carboxamide and propanamide derivatives bearing phenylpyridazine as a core ring and the investigation of their inhibitory potential on in-vitro acetylcholinesterase and butyrylcholinesterase. Bioorg Chem. 2018; 79: 235-249. https://doi.org/10.1016/j.bioorg.2018.05.006

[28] Kilic B, Gulcan HO, Yalcın M, Aksakal F, Dimoglo A, Sahin MF. Synthesis of some new 1 (2H)-Phthalazinone derivatives and evaluation of their acetylcholinesterase and butyrylcholinesterase inhibitory activities. Lett Drug Des Discov. 2017; 14(2): 159-166. https://doi.org/10.1007/s00044-014-1205-8

[29] Yamali C, Gulcan HO, Kahya B, Cobanoglu S, Sukuroglu MK, Dogruer DS. Synthesis of some 3(2H)-pyridazinone and 1(2H)-phthalazinone derivatives incorporating aminothiazole moiety and investigation of their antioxidant, acetylcholinesterase, and butyrylcholinesterase inhibitory activities. Med Chem Res. 2015; 24(3): 1210-1217. https://doi.org/10.1007/s00044-014-1205-8

[30] Bardakkaya M, Kilic B, Sagkan RI, Aksakal F, Shakila S, Dogruer DS. Synthesis and evaluation of multitarget new 2-aminothiazole derivatives as potential anti-Alzheimer's agents. Arch Pharm. 2023; 356(8): 2300054. https://doi.org/10.1002/ardp.202300054

[31] Ostrowska K. Coumarin-piperazine derivatives as biologically active compounds. Saudi Pharm J. 2020; 28(2): 220-232. https://doi.org/10.1016/j.jsps.2019.11.025

[32] Bajda M, Wieckowska A, Hebda M, Guzior N, Sotriffer CA, Malawska B. Structure-based search for new inhibitors of cholinesterases. Int J Mol Sci. 2013; 14(3): 5608-5632. https://doi.org/10.3390/ijms14035608

[33] Abouel-Enein SA, Emam SM, Abdel-Satar EM. Bivalent metal chelates with pentadentate azo-schiff base derived from nicotinic hydrazide: preparation, structural elucidation, and pharmacological activity. Chem Biodivers. 2023; 20(6): e202201223. https://doi.org/10.1002/cbdv.202201223

[34] Cao L, Zhang L, Cui P. Synthesis of 3-(3-Alkyl-5-thioxo-1H-4,5-dihydro-1,2,4-triazol-4-yl)aminocarbonylchromones. Chem Heterocycl Compd (NY). 2004; 40(5): 635-640. https://doi.org/10.1023/B:COHC.0000037320.27881.27

[35] Munir R, Javid N, Zia-ur-Rehman M, Zaheer M, Huma R, Roohi A, Athar Mm. Synthesis of novel N-acylhydrazones and their C-N/N-N bond conformational characterization by NMR spectroscopy. Molecules. 2021; 26(16): 4908. https://doi.org/10.3390/molecules26164908

[36] Palla G, Predieri G, Domiano P, Vignali C, Turner W. Conformational behaviour and E/Z isomerization of N-acyl and N-aroylhydrazones. Tetrahedron. 1986; 42(13): 3649-3654. https://doi.org/10.1016/S0040-4020(01)87332-4

[37] Bortolami M, Pandolfi F, De Vita D, Carafa C, Messore A, Di Santo R, Feroci M, Costi R, Chiarotto I, Bagetta D, Alcaro S, Colone M, Stringaro A, Scipione L. New deferiprone derivatives as multi-functional cholinesterase inhibitors: design, synthesis and in vitro evaluation. Eur J Med Chem. 2020; 198: 112350. https://doi.org/10.1016/j.ejmech.2020.112350

[38] Liu Y, Di Y, Liu M, Qiao C, Gao X, Zhou C. Synthesis, thermodynamic properties and Hirshfeld surface analysis of 2-[(4-methyl-benzoyl)-hydrazone]-propionic acid. J Mol Struct. 2022; 1260: 132792. https://doi.org/10.1016/j.molstruc.2022.132792

[39] Selvam P, Sathiyakumar S, Srinivasan K, Premkumar T. A Copper(II) complex of a new hydrazone: A solid-state single source precursor for the preparation of both Cu and CuO nanoparticles. J Mol Struct. 2019; 1177: 469-475. https://doi.org/10.1016/j.molstruc.2018.09.082

[40] Purandara H, Raghavendra S, Foro S, Patil P, Gowda BT, Dharmaprakash SM, Vishwanatha P. Synthesis, spectroscopic characterization, crystal structure, Hirshfeld surface analysis and third-order nonlinear optical properties of 2-(4-chlorophenoxy)-N'-[(1E)-1-(4-methylphenyl) ethylidene] acetohydrazide. J Mol Struct. 2019; 1185: 205-211. https://doi.org/10.1016/j.molstruc.2019.02.079

[41] Schrödinger Release 2021-3: QikProp, Schrödinger, LLC, New York, NY, 2021.